Journal of Intelligent & Robotic Systems (2022) 106:66
https://doi.org/10.1007/s10846-022-01765-3

SHORT PAPER

Modeling and Design of a Stair Climbing Wheelchair with Pose Estimation and Adjustment

Bibhu Sharma[1] · Branesh M. Pillai[1] · Korn Borvorntanajanya[1] · Jackrit Suthakorn[1]

Received: 21 April 2022 / Accepted: 27 October 2022

Abstract
Urban locomotion is a challenge for individuals with lower limb impairment or any other conditions that inhibit ambulation. While wheelchairs are the absolute choice, they do not address the entire problem of accessibility in urban locomotion despite the use of actuators. One of the viable prospects has been demonstrated by Stair Climbing Wheelchairs (SCW), which rely on different modes of mechanism to traverse the staircase. Since staircases are the most common and one of the challenging elements of the urban setting, these wheelchairs are supposed to sufficiently address the problems of the terrain. However, several technical and psychological shortcomings hinder a wider practical use. This paper discusses semi-autonomous tracked SCW and introduces a novel kinematic mechanism design that facilitates successful switching of the mode of locomotion and autonomous pose adjustment with the changing terrain. To execute the intended task of pose estimation/adjustment and variable locomotion, an algorithm that combines multiple sensor data with the kinematic model has been developed. The developed prototype was tested in a loaded condition in staircases of different gradients. The experimental results suggest that the system addresses a plethora of issues mentioned in the literature, considering the factors of accessibility and safety. Also, this paper has highlighted the requirement of vibration suppression for user comfort, promoting technological acceptance and adaptation.

Keywords Rehabilitation robotics · Kinematic design · Stair-climbing

1 Introduction

1.1 Motivation

Recent years have seen unprecedented growth in the size of the personal mobility devices (PMD) market, estimated to be around USD 11.5 billion in 2020 [1]. The rise in the global geriatric population, in addition to enhanced technological development and acceptance, are some of the contributing factors. Undoubtedly, within the overall PMD market, powered wheelchair occupies a significant portion.

Regardless of the prevalent market size for the powered wheelchair, there exist several factors that are detrimental to its usage. One of the biggest impediments to the vast majority of PMDs is the issue of accessibility. As these devices rely primarily on the wheels, the design of the infrastructures mostly disregards the consideration of the PMD users. The problem of accessibility is still seen at large by the majority of wheelchair users around the world [2, 3]. Another major issue associated with PMD is the notion of safety. According to a survey, 21% of power wheelchair users reported physical accidents [2]. Another survey indicated that 19% of the users lacked a 'sense of safety' and felt vulnerable during usage [4]. While quantification and analysis of physical safety are convenient, the comprehension of the psychological aspects is intricate [5]. Thus, regarding the wider use and acceptance of PMD for urban locomotion, enhancing accessibility while ensuring physical as well as psychological safety is pivotal.

✉ Jackrit Suthakorn
jackrit.sut@mahidol.ac.th

Bibhu Sharma
sharmabibhu2@gmail.com

Branesh M. Pillai
branesh.mad@mahidol.ac.th

Korn Borvorntanajanya
korn@bartlab.org

[1] Center for Biomedical and Robotics Technology (BART LAB), Faculty of Engineering, Mahidol University, Salaya, Phutthamonthon 73170, Nakorn Pathom, Thailand

Published online: 17 November 2022

1.2 Related Work

The prevalence of stair climbing PMDs is significantly scarce when compared to other PMDs. Still, several approaches exist within the research and commercial sphere to address the issue. Tao et al. have classified the prevalent methods of stair climbing for wheelchairs into four classes: leg-based, wheel cluster-based, hybrid and tracked [6]. Leg-based stair climbing method relies on the mechanical actuated leg-like features to climb the stairs [7–9]. Similarly, in a wheel cluster-based mechanism, multiple wheels in multiple axes are arranged in a planetary formation along a single axis, such that the normal locomotion is served by a rotation of the wheels and climbing is ensured by revolution along the common axis [10–16]. While three wheeled-cluster [11–14, 17] or hex wheeled-cluster [18] are mechanically stable, two-wheeled-cluster mechanisms rely on an inverted pendulum-type control method to maintain dynamic stability [15, 16].

A hybrid mechanism refers to a general class of methods involving a combination of leg and wheel combined with a kinematic configuration to ensure rolling and climbing [19–25]. While [19] mentions the use of rolling legs for climbing, [20] combined normal wheels with adjustable wheeled legs to perform the same task. Another hybrid design involving powered omnidirectional wheels within a system of four-bar linkage legs has been demonstrated in [22–24]. Mostyn et al. [21] proposed the variable-shaped wheels that are adjusted for stair locomotion and normal locomotion. Apart from these, several unconventional methods including user operated lever which propels the rotary legs have been described in the literature [26].

Compared to the aforementioned methods, tracked locomotion mechanism is considered to have simpler design and control dynamics [27]. A model with variable geometry tracked flippers has been laid out by [28], which adjusts according to the terrain. The design of stair-climbing wheelchair switching between normal locomotion powered by wheel hub and tracks has been demonstrated by [29, 30]. The designs utilize a kinematic switching mechanism to select the mode of locomotion and adjust the angles. Some stair climbing wheelchairs are also designed with only tracked locomotion system [31].

In addition to the mechanical design, the control aspect of PMD is pivotal for the performance. Assistive devices of this kind predominantly utilize a type of human-in-the-loop method [32–35], which fundamentally combines the autonomous and manual method. As the user commands the device for locomotion, the pose adjustment, navigation, and mapping are generally automated. Instead of physical command from the user, even brain signal has been used to control smart wheelchairs [32, 36].

Regarding navigation and mapping, the use of an accelerometer sensor and gyroscopic sensor along with Kalman filter sensor fusion with the conventional dead reckoning algorithm was proposed in a lunar rover [37]. This was also used by [38], where a proprioceptive angular transducer sensor was used to estimate tilt while the co-ordinates and heading angles were estimated by the conventional odometry. A similar approach was used by [39], where a combined adaptive and extended Kalman filter was used along with the proprioceptive sensors to estimate the center of gravity of the robot. Along with the class of sensors, tracked robots frequently use visual sensors for accurate estimation. For example, [40] uses an on-board camera to estimate the heading angle of the staircase. Even for a powered wheelchair, [41] uses convolutional neural network to recognize the environment for automated navigation, while stochastic methods considering Gaussian distribution have also been used for location and heading estimation [42, 43]. Moreover, pose estimation of the tracked robots using conventional odometry and current sensing based on disturbance observer feedback has been discussed in [44, 45].

As papers mentioned above discusses locomotion system, pose estimation/adjustment system or the control system, there are several works in literature that discusses the entire system. One of the commonalities is the use of planar LIDAR rangefinder to detect and measure the architectural barrier such as staircase [46–48]. While [49] illustrates a system incorporating ultrasonic sensor to detect the staircase. After the staircase is detected, [46] illustrates a model with cluster-wheel mechanism integrated with the system in a kinematic chain, such that the pose adjustment and locomotion occurs simultaneously. Similar kinematic chain is illustrated in [47, 48], but for a hybrid leg-wheel system that performs pose estimation and adjustment in real-time. Comparing with these designs, [49] discusses an unconventional method which combines a powered wheelchair with supporting dual mobile manipulator that pushes the robot along the staircase utilizing the kinematic model. Another approach has been illustrated in [50] which controls the active tension of the belt in tracked wheelchair robot to adjust the pose and does not require any pose estimation method.

Although a plethora of works demonstrate different approaches to address the problem, there still exist significant limitations. For example, the inverted pendulum-based stair climbing wheelchair (SCW) requires human assistance or a handrail to maintain stability [51]. In addition, they require high energy to maintain the balance of the center of gravity (CG). Even though this shortcoming has been addressed in [15], the climb duration is nearly 24 seconds per step, making the overall climb duration to be quite high. Compared to the model, the three-wheeled SCW offers stability and does not require any human or physical assistance.

However, due to a fixed arrangement of the wheels, the robot encounters intricacies when approaching obstacles of varying sizes, which are commonalities for urban terrain. This might not be an issue for wheel-leg hybrid SCWs, but motion planning is a challenge for these robots since they require high degrees of freedom (DOF) to execute safe climbing process. Moreover, the overall length of hybrid robots such as illustrated in [20, 25] is greater than the standard wheelchair size, making them difficult to turn in a confined space. In addition, the complexity of motion planning slows down the obstacle-overcoming process [20]. However, the shortcomings that are mentioned are not relevant for tracked robots, serving practical purpose [27, 51]. But tracked robots face challenges such as higher weight, low tip-over stability due to fewer points of contact, and a requirement for a higher degree of freedom for CG balance [14]. However, when compared to [46] and [47], after the visual sensing system detects the staircase, kinematic chain involving tracked robots have fewer control variables, making system convenient and ensures lower computational cost.

1.3 Contribution

With the goal of addressing safety and accessibility in urban scenario, this paper discusses the design and modeling of the SCW, while avoiding the pitfalls associated with other similar robotic technologies. Specifically, the paper discusses the design and development of a novel hybrid track-based mobility system consisting of a pose estimation/adjustment system. The pose estimation system utilizes the sensor data from inertial measurement unit (IMU) and combines with the feedback from the actuators to accurately estimate and adapt the robot to the challenges of the terrain. The contribution of this research, based on the prevalent state of technology and literature are as follows:

1. This research has developed a novel design of a robotic wheelchair that can traverse various obstacles in urban settings including staircases of uniform as well as variable dimensions. The intended execution is within the optimum time duration without necessitating physical or human assistance. By optimizing the kinematic and kinetic range of performance, higher load can be handled with a light-weight design, thus addressing the goal of accessibility
2. With the human-in-the-loop control method, by ensuring human of having maximum control over the locomotion and automating the adjustment function, the psychological aspect of technological adaptation is ensured.
3. The developed kinematic model along with the differential odometry, when combined with the pose estimation and adjustment system consisting of IMU and LIDAR has profound application for 3D navigation in autonomous and semi-autonomous systems. The forward kinematics evaluation, consisting of closed form solution, offers real-time calculation with safe and reliable but lower computational cost.
4. The overall research attempts to comply with ISO 7176:28:2012, which is a standard for stair-climbing devices that climb from a backward direction. This is to ensure and elevate safety, acceptability and commercialization.

2 Kinematic Modeling

Basically, the system combines the mobility components with an adjustment components along with the physical interface for the user. As mentioned, the wheelchair utilizes normal locomotion (a wheel with hub motor) and tracked locomotion, based on the terrain. This transition is facilitated by an adjustment system which relies on linear actuators. Ultimately, the actuators within both the mobility and adjustment components induce changes in the state matrix where (x, y, z) refers to the change in 3D co-ordinates and ϕ refers to the attitude angle with reference to a fixed world frame. The components are organized according to the layout as shown in Fig. 1.

In order to analyze the motion, the first step is to postulate the kinematic relationship between the actuators and the overall system. As such, the effects of hub motor, track motor and linear actuators have to be articulated. The kinematic relation corresponding to the mobility components has been formulated through the concept of dead reckoning. However, contrary to the widely used dead reckoning calculation in two-dimension, modified three-dimension dead reckoning

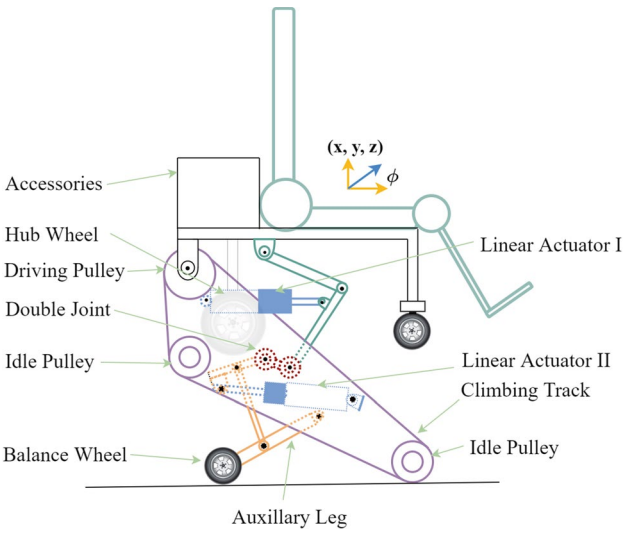

Fig. 1 Outline of the stair climbing wheelchair along with the components

relation has to be developed as per the intended motion plan. The calculation and estimation would rely entirely on the estimation of the wheelchair posture, based on the kinematic effect of the linear actuator displacement. Therefore, in this section, a forward kinematic relation between the control variables and the state variables would be formulated, followed by the 3D dead reckoning algorithm. The conclusion of the section would be a broad relationship between the control variables and accurate estimation of the position and the posture of the mobility system.

2.1 Forward Kinematic Formulation

To comprehend the geometry of the problem, the layout as demonstrated in Fig. 1, has been simplified as a basic diagram as shown in Fig. 2. Within the forward kinematic section, the main objective is to map the relation between the linear displacements s_1 and s_2 with the state variables (x, y, z, ϕ). Even though the calculation is straightforward, the presence of several passive links adds complexity to the analysis. The diagram is further simplified as each linear actuator chain is isolated and analyzed. Besides, a couple of intermediate angles θ_1 (angular displacement of chair base with track) and θ_2 (angular displacement of the auxiliary leg) are defined to further ease the analysis process.

It is evident from Fig. 3 that the contraction of the linear actuator 2 increases θ_2 and the extension rotates the auxiliary leg towards the home position. Considering O (front end of the track) as a fixed fulcrum and A as a sliding link, the links OP and AB form a sort of modified Scott-Russel mechanism. This linkage is different from a conventional Scott-Russel mechanism due to two reasons: 1) the arrangement of the links is different, and joint B lies within the link OP. 2) link AB is supposed to be half of the link OP. Due to the difference, we term this as a modified Scott-Russel mechanism and contrary to the exact straight line output of joint P in a conventional Scott-Russel mechanism, joint P produces a nonlinear motion. As mentioned, the main objective of this section is to determine the relationship between the linear displacement of the linear actuator and the impact on the

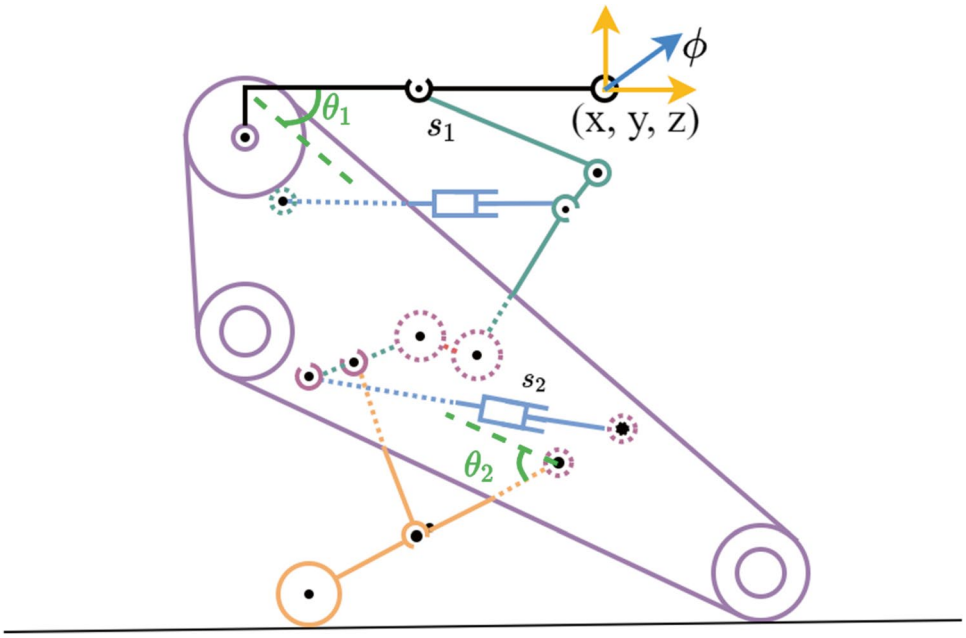

Fig. 2 Simplified diagram for the forward kinematics analysis

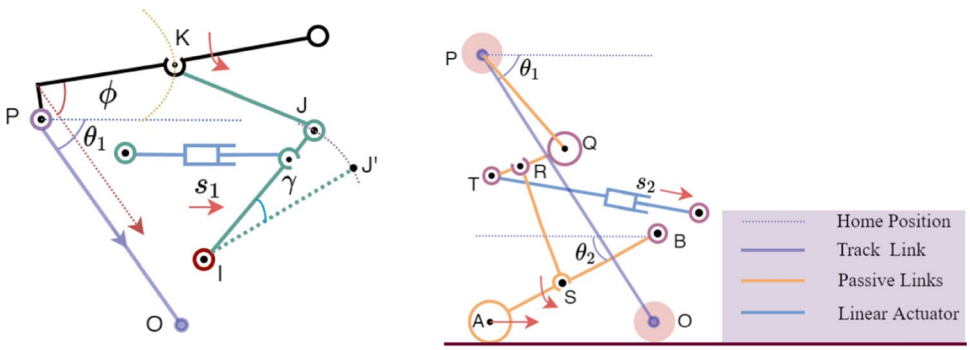

Fig. 3 Kinematic loop around the linear actuators I and II and the relation with the overall system

overall posture of the wheelchair. The kinematic chain maintained by the linear actuator 2 can be analyzed in two steps:

1. Determine the effect of s_2 on the rotation θ_2 which is the angular displacement of the auxiliary leg.
2. From θ_2 determining the angle θ_1 which is the angular displacement of the track link from the initial position.

For step 1, it is clear that the link QT rotates with the center at Q when the linear actuator slides. Also, as links QT and AB are designed to be parallel, both the links have the same angular displacement: θ_2. In the triangle formed by QTT', cosine law can be implemented as follows:

$$TT' = \sqrt{QT^2 + QT'^2 - 2QT \times QT' \times cos\theta_2} \tag{1}$$

Since, QT and QT' both represents same link at mere different instance, both the parameters are equal (consider QT=r). From Eq. 1,

$$TT'^2 = 2r^2\left(1 - cos\theta_2\right) \tag{2}$$

Figure 3 can be represented with more geometric details as Fig. 4 for the purpose of analysis. Here, LT and LT' are the initial and final positions of the linear actuator 2. Cosine Law can again be implemented in triangle QT'L.

$$TT' = \sqrt{LT^2 + QL^2 - 2LT \times QL \times cos\gamma} \tag{3}$$

Here, γ is the angle made by the linear actuator during the motion. To find the relation between the linear displacement s_2 and the angular displacement of the link QT (θ_2), γ has to be determined. This can be done through triangle QT'L as:

$$r^2 = LT'^2 + QL^2 - 2LT' \times QL \times cos(\gamma + \angle QLT) \tag{4}$$

From Eq. 4, γ can be calculated as:

$$\gamma = cos^{-1}\left\{\frac{QL^2 + LT'^2 - r^2}{2LQ.OT'}\right\} - \angle QLT \tag{5}$$

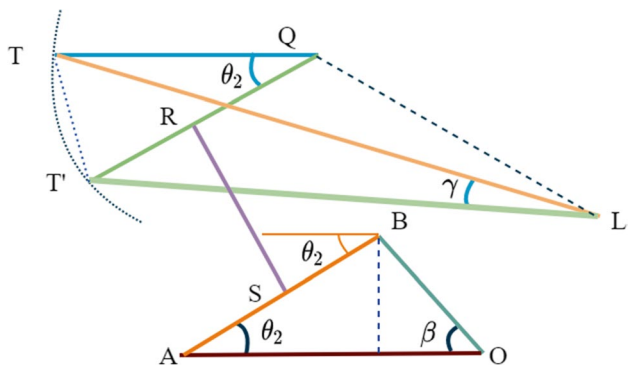

Fig. 4 Kinematic loop simplification for comprehension

The Eqs. 2 and 3 can be equated as:

$$2r^2\left(1 - cos\theta_2\right) = LT^2 + QL^2 - 2LT \times QL \times cos\gamma \tag{6}$$

But the definition of γ has been determined from Eq. 5, which can be plugged into Eq. 6. Consequently, Eq. 6 can be rewritten for mapping the relationship between the angular displacement and the linear displacement as:

$$\theta_2 = cos^{-1}\left\{1 - \frac{LT^2 - LT'^2 - 2LT.LT'cos\angle QLT}{2r^2} + LT.\frac{LT^2 + LT'^2 - r^2}{2r^2LQ}\right\} \tag{7}$$

From Fig. 4, it is evident that the angular displacement of QT is propagated equally to the link AB because of the link RS. Therefore, in AOB, we consider $\angle BOA$ to be β, where, $\beta = \theta_1 + \angle BOP$ It is worth noting that the points B, O and P are static within the track frame, $\angle BOP$ is constant throughout the motion and in fact is a design parameter. We construct a line BB' perpendicular to line AO. Using trigonometric rules:

$$BB' = OBsin\beta = ABsin\theta_2 \tag{8}$$

which can also be written as, $sin\beta = \frac{AB}{OB}sin\theta_2$.

From Eq. 4,

$$sin\left(\theta_1 + \angle BOP\right) = \frac{AB}{OB}sin\theta_2 \tag{9}$$

Therefore,

$$\theta_1 = sin^{-1}\left(\frac{AB}{OB}sin\theta_2\right) - \angle BOP \tag{10}$$

The parameter θ_1 mentioned in the above equation is the tilt of the track axis from the initial position. The expression of θ_1 from Eq. 10 and the expression of θ_2 from Eq. 7 have been plotted against the linear actuator displacements in Fig. 5. The angles are observed to be progressing nonlinearly along the increase in linear actuator displacement. However, the objective of the forward kinematic formulation is to ultimately determine the position and orientation of the chair frame. This cannot be calculated without considering the linear displacement of the linear actuator 1. Similar to the kinematic chain around linear actuator 2, a similar kinematic chain drawing has been prepared for linear actuator 1. In Fig. 3, the angle ϕ is the total angular displacement of the chair link from the initial position. However, it is composed of two parts: $\phi = \theta_1 + \gamma$ Let us consider γ to be the angular displacement in link IJ as shown in the figure. Similarly, during the motion, let us suppose that point J is displaced to J'. Using cosine law in the triangle formed by IJJ':

$$JJ' = \sqrt{IJ^2 + IJ'^2 - 2IJ \times IJ' \times cos\gamma} \tag{11}$$

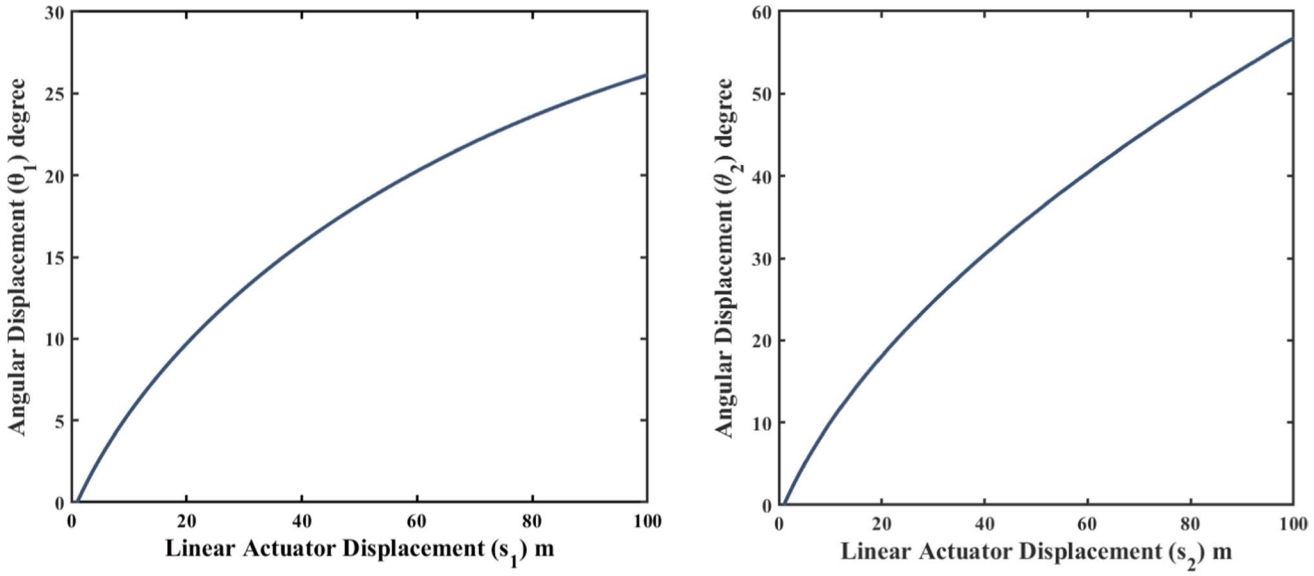

Fig. 5 Angular variation with respect to the linear actuator displacement

The length JJ' is a direct outcome of the linear displacement of the linear actuator therefore the parameter s_1 is equal to the length JJ'. Also, IJ and IJ' are both the same links. Therefore,

$$s_1^2 = IJ^2 + IJ^2 - 2IJ^2 cos\gamma \tag{12}$$

Which gives,

$$\gamma = cos^{-1}\left(1 - \frac{s_1^2}{2IJ^2}\right) \tag{13}$$

Finally, the tilt of the chair ϕ can be calculated from Eqs. 10 and 13 as:

$$\begin{aligned}\phi = & f(s_1, s_2) = \left(\frac{AB}{OB} sin\left(1 - \frac{s_2^2}{2QT^2}\right)\right) - \angle BOP \\ & + cos^{-1}\left(1 - \frac{s_1^2}{2IJ^2}\right)\end{aligned} \tag{14}$$

As a clear mathematical relation is defined between the tilt angle ϕ and the linear displacement of both the actuators, according to our initial definition of forward kinematics, the relation of the linear displacement of actuators with the coordinates of any arbitrary point within the chair frame has to be determined. However, this analysis is simplified because of the fact that (x, y, z, ϕ) are bound by the holonomic constraints, which means that the parameters (x, y, z) can be expressed in the terms of ϕ. Since the system can be represented with a planar robot, it lacks any motion along the y-direction. Therefore, the displacement of the intended point $V(x, z)$ can be determined as:

$$\begin{aligned} x &= ABcos\theta_2 + PVcos\phi \\ z &= ABsin\theta_2 + PVsin\phi \end{aligned} \tag{15}$$

Despite a clear relation between s_1, s_2 and (x, y, z, ϕ) is developed, this is incomplete because the behavior of the linear displacement of the actuator on the chair frame is different within the different bounds of the angles ϕ and θ_2. Different scenarios based on the bounds on the angle have been demonstrated in Fig. 6. The scenarios would be explored independently in both cases and combined later for a general equation that maps the linear actuator displacement with the effect on the end-effector.

Case 1: For the variation in the goal pose, the angular displacement θ_1 should surpass a certain threshold defined by the design parameters. The main design parameter that affects the threshold is the vertical distance of the track from the ground plane, shown as OG_2 in Fig. 8. Basically, the threshold refers to the angle θ_1 when the track pulley at point O has contact with the floor.

$$\theta_1^{threhold} = sin^{-1}\left(\frac{OG_2}{OP}\right) \tag{16}$$

Therefore,

$$\phi = \begin{cases} 0 & if, \theta_1 < \theta_1^{threshold} \\ f(s_1, s_2) & if, \theta_1 > \theta_1^{threshold} \end{cases} \tag{17}$$

Here, $f(s_1, s_2)$ is the expression from the Eq. 14.

Case 2: As shown in Fig. 6, the impact of the change in angular displacement θ_2 on the pose of the chair frame initiates when the angular displacement crosses a certain threshold (similar to case 1). Here, the design parameter

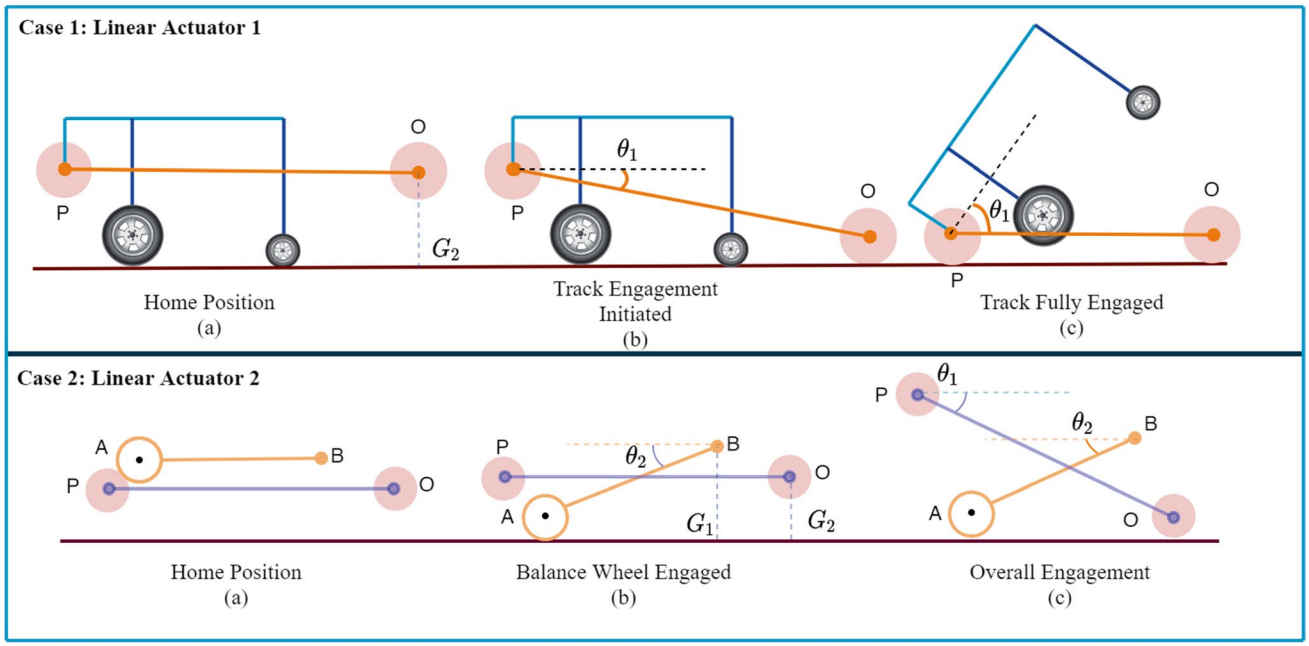

Fig. 6 Relation between linear actuator activity and posture adjustment of wheelchair

that determines the threshold angle is the distance of the fulcrum B from the ground (represented by BG1) and the length of the auxiliary balance wheel arm AB.

$$\theta_2^{threhold} = sin^{-1}\left(\frac{BG_1}{AB}\right) \tag{18}$$

Therefore,

$$\phi = \begin{cases} 0 & if, \theta_2 < \theta_2^{threshold} \\ f(s_1, s_2) & if, \theta_2 > \theta_2^{threshold} \end{cases} \tag{19}$$

Finally, Eqs. 17 and 19 can be combined into a function that takes into account the overall bounds.

$$\phi = \begin{cases} 0 & if, \theta_1 < \theta^{threshold} \text{ and } \theta_2 < \theta_2^{threshold} \\ f(s_1, s_2) & if, \theta_1 > \theta^{threshold} \text{ and } \theta_2 > \theta_2^{threshold} \end{cases} \tag{20}$$

Also, the relation can be plotted as a surface plot which maps the relationship between the linear displacement of the two actuators and the absolute orientation of the chair frame as in Fig. 7.

The mapping of Fig. 7 can be observed in simulation through the use of CAD model of proposed robot when climbing staircase as shown in Fig. 8. While the robot pose adjustment is controlled through kinematic chain driven by the linear actuators, the intended pose can be observed to be appropriate to climb an arbitrary staircase. Moreover, the balance wheel which is driven by one of the linear actuator-based kinematic chain, operates appropriately to reduce the landing jerk and maintain the stable position of the CG, as demonstrated in Fig. 8d. Moreover, the simulation ensures that the theoretical model can be used to maintain the 3D pose of the robot in all the modes from initiation to climb completion, further corroborating the utility of the mechanical and mathematical model.

2.2 Forward Kinematics: 3D Dead Reckoning

Generally, the pose (position + orientation) estimation and measurement are performed in robots with the dead-reckoning algorithm. It is a relative pose estimation method and it does not require expensive sensors to measure and operates with significant accuracy. Basically, it measures the rotation of the wheels and the amount of the rotation is mapped to the change in relative pose of the robot. Obviously, this measurement consists of error, which demands inertial information to compensate for the tracking error, therefore IMU sensors are used. However, most of the applications of the dead-reckoning algorithm is performed by considering a 2D World Frame. Therefore, the variables that are observed are (x, y) co-ordinate of the robot-frame and altitude angle ψ which gives the angle made by a robot with the World Frame. But this level of implementation is insufficient in our case because the robot is intended to operate mainly in a 3D environment and estimation in a 3D frame is absolutely necessary. Therefore, we propose a 3D dead-reckoning algorithm that is specific to our application. To bring into perspective, two views of the robot operation are demonstrated in Fig. 8.

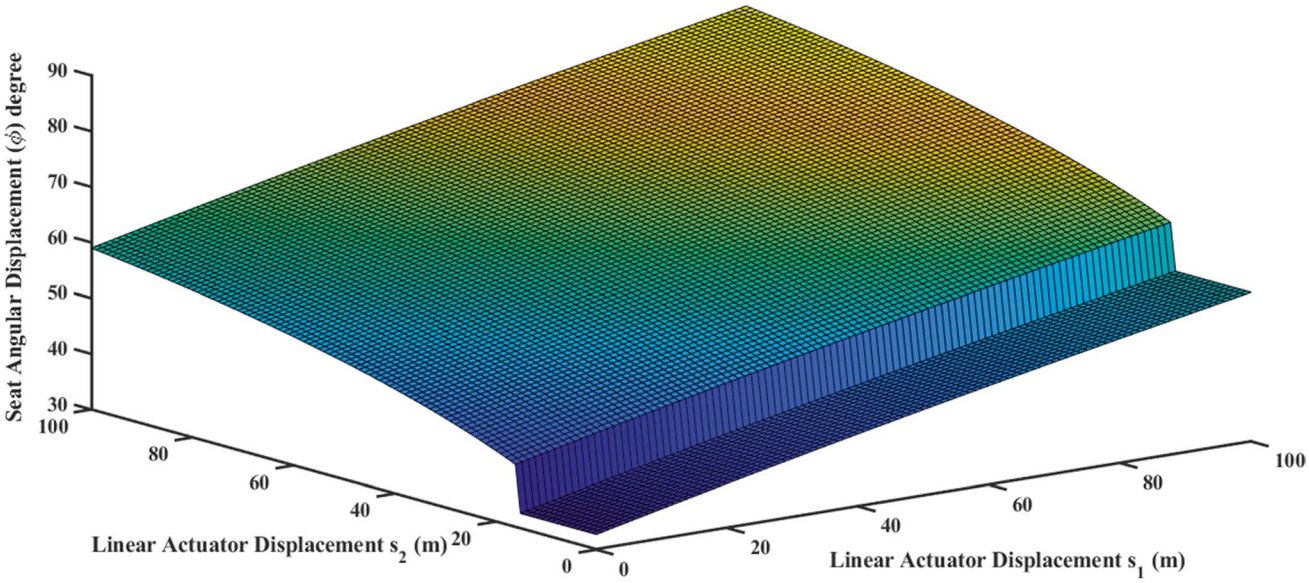

Fig. 7 Variation of Seat angle ϕ with respect to s_1 and s_2

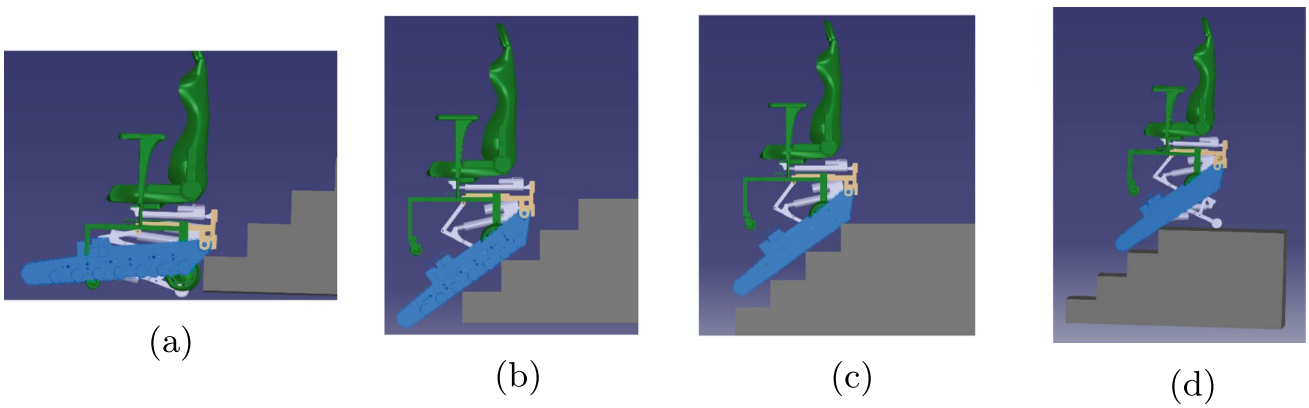

Fig. 8 CAD-based Simulation of the proposed mechanical model with the mathematical model that executes the two kinematic chains actuated by two linear actuators. (**a**) Approach, (**b**) Initiate climb-up, (**c**) Climbing and (**d**) Balance mode

The main aim of the process is to find the transformation of the robot frame with different frames as mentioned. Let us assume the transformation between the world frame and the base frame is denoted as T_{base}^{World}. It is evident from the supposition that the base frame has exactly the same orientation as that of the world frame and is merely a translation. At first, to extract the position information, the velocity of the base frame (v_b) has to be determined using the velocity of the track (v_t). The velocity of the track is related to the angular velocity of the driven pulley (ω_l, ω_r), which can be calculated by differentiating the encoder readings (E_l, E_r) of the motors with respect to the sampling time T_s (Fig. 9).

$$\omega_l = \frac{E_l^{final} - E_l^{initial}}{T_s} \cdot \frac{\pi}{180} \cdot Q(rad/\sec) \tag{21}$$

$$\omega_r = \frac{E_r^{final} - E_r^{initial}}{T_s} \cdot \frac{\pi}{180} \cdot Q(rad/\sec) \tag{22}$$

The multiplying factor Q is related to the gear ratio of the spur gearhead (G_g) and the gear ratio of the driving and the driven pulleys (G_p).

$$Q = \frac{1}{G_g \times G_p} \tag{23}$$

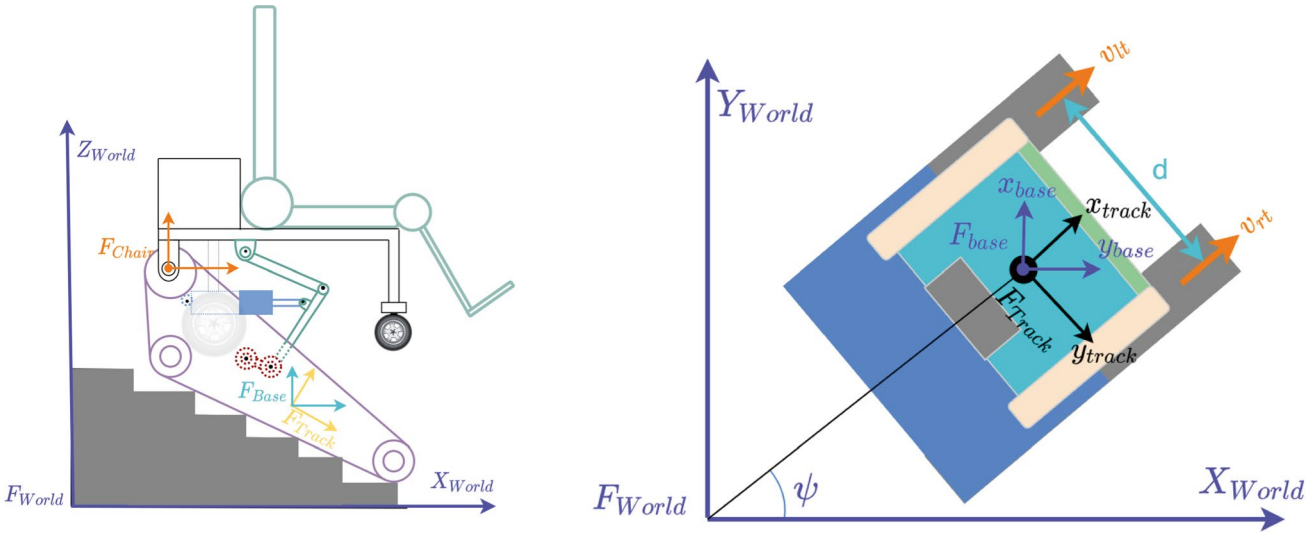

Fig. 9 Kinematic loop around the linear actuators I & II and the relation with the overall system

Algorithm 1 Staircase detection algorithm using LIDAR

Require: *Coordinates* from LIDAR
  Run Harris Corner Detection Algorithm on *Coordinates*
  if Distance between Points is equal **then**
    Update *PointArray*
  end if
  Polynomial Curve Fitting of *PointArray*
  Find the $Slope\_of\_Curve(PointArray)$
  if $Slope\_of\_Curve \neq 0$ **then**
    Return *StaircaseDetection*=True
    Return ϕ_{goal}=$tan^{-1}(Slope\_of\_Curve)$
    Return *StaircaseLength* = Length of Polynomial Curve
    if $\phi_{goal} < 0$ **then**
      Return $ClimbingMode = ClimbingUp$
    else if $\phi_{goal} > 0$ **then**
      Return $ClimbingMode = ClimbDown$
    end if
  end if

The angular velocity can be used to calculate the left and right track velocities as:

$$v_{lt} = \omega_l \times l_t \tag{24}$$

$$v_{rt} = \omega_r \times l_t \tag{25}$$

where l_t is the length of the track. The linear velocity (v_t) of the track frame with respect to the world frame can thus be calculated as:

$$v_t = \frac{v_{lt} + V_{rt}}{2} \ (meter/\sec) \tag{26}$$

Let ${}^{i}q_b({}^{i}x_b, {}^{i}y_b, {}^{i}z_b)$ be the initial position of base and ${}^{f}q_b({}^{f}x_b, {}^{f}y_b, {}^{f}z_b)$ be the final position of base. The variation in each of the co-ordinates can be written as:

$$\begin{aligned} {}^{f}x_b &= {}^{i}x_b + v_t T_s cos\psi cos\sigma \\ {}^{f}y_b &= {}^{i}y_b + v_t T_s sin\psi cos\sigma \\ {}^{f}z_b &= {}^{i}z_b + v_t T_s sin\sigma \end{aligned} \tag{27}$$

Regarding the angular velocity of track frame, there are two angular velocity components that requires consideration: angular velocity w.r.t. z_{base}: ω_t^{yaw} and angular velocity w.r.t. y_{base}: $\omega_t^{y_{base}}$.

Algorithm 2 Staircase climbing Algorithm combining kinematic model with the sensor data from IMU and LIDAR

Require: $UserCommand, StaircaseDetection, \phi_{measure}, StaircaseLength$
  $\phi_{measure} \leftarrow x_{rotation}$ from IMU
  if $StaircaseDetection = False$ **then**
    Move HubMotor as $UserCommand$
  else if $StaircaseDetection = True$ **then**
    Calculate $s_{1,goal}$ and $s_{2,goal}$ from Eq. 20
    while $\phi_{measure} < \phi_{goal}$ **do**
      if $s_{1,measure} < s_{1,goal}$ & $s_{2,measure} < s_{2,goal}$ **then**
        $s_1 \leftarrow s_1 + 1$
        $s_2 \leftarrow s_2 + 1$
      end if
    end while
    if $\psi_{measure} < StaircaseWidthDirection$ **then**
      /* Wheelchair Alignment Adjustment */
      $\omega_t^{yaw} \leftarrow \omega_t^{yaw} + 1$ from Eq. 28
    else if $\psi_{measure} > StaircaseWidthDirection$ **then**
      $\omega_t^{yaw} \leftarrow \omega_t^{yaw} - 1$ from Eq. 28
    end if
    while $StaircaseTravelLength \neq StaircaseLength$ **do**
      Rotate Track Motor as $UserCommand$
    end while
    /* End of Staircase */
    Increment s_2 until $\omega_{measure}$ increases for Normal Locomotion
  end if

$$\begin{aligned}\omega_t^{yaw} &= \frac{v_{lt} - v_{rt}}{d}\ (rad/sec)\\ \omega_t^{pitch} &= \frac{d\sigma}{dt}\ (rad/sec)\end{aligned} \tag{28}$$

To mathematically define the transformation between different frames, a transformation matrix (**T**) can be defined between the frames involved. First of all, from the definition, the homogeneous transformation matrix between the world frame and the base frame can be calculated by considering just the translation of the base frame from the world reference frame.

$$\mathbf{T}_{\text{Base}}^{\text{World}} = \begin{bmatrix} 1 & 0 & 0 & x_b \\ 0 & 1 & 0 & y_b \\ 0 & 0 & 1 & z_b \\ 0 & 0 & 0 & 1 \end{bmatrix} \tag{29}$$

While $\mathbf{T}_{\text{Base}}^{\text{World}}$ represents pure translation from the World frame to the Base frame, the transformation between the base frame and the track frame ($\mathbf{T}_{\text{Track}}^{\text{Base}}$) is represented by the two rotations: pitch and yaw. Therefore, $\mathbf{T}_{\text{Base}}^{\text{World}}$ accounts for translation and $\mathbf{T}_{\text{Track}}^{\text{Base}}$ represents rotation of the robot with the absolute World frame. $\mathbf{T}_{\text{Track}}^{\text{Base}}$ is given as:

$$\begin{aligned}\mathbf{T}_{\text{Track}}^{\text{Base}} &= \begin{bmatrix} cos\psi & 0 & sin\psi & 0 \\ 0 & 1 & 0 & 0 \\ -sin\psi & 0 & cos\psi & 0 \\ 0 & 0 & 0 & 1 \end{bmatrix}^{pitch} \times \begin{bmatrix} cos\sigma & -sin\sigma & 0 & 0 \\ sin\sigma & cos\sigma & 0 & 0 \\ 0 & 0 & 1 & 0 \\ 0 & 0 & 0 & 1 \end{bmatrix}^{yaw} \\ &= \begin{bmatrix} cos\psi cos\sigma & -cos\psi sin\sigma & sin\psi & 0 \\ sin\sigma & cos\sigma & 0 & 0 \\ -sin\psi & sin\psi sin\sigma & 0 & 0 \\ 0 & 0 & 0 & 1 \end{bmatrix}\end{aligned} \tag{30}$$

Therefore, the transformation between world frame and track frame can be determined as:

$$\mathbf{T}_{\text{Track}}^{\text{World}} = \mathbf{T}_{\text{Base}}^{\text{World}} \times \mathbf{T}_{\text{Track}}^{\text{Base}} = \begin{bmatrix} cos\psi cos\sigma & -cos\psi sin\sigma & sin\psi & x_b \\ sin\sigma & cos\sigma & 0 & y_b \\ -sin\psi & sin\psi sin\sigma & 0 & z_b \\ 0 & 0 & 0 & 1 \end{bmatrix} \tag{31}$$

The transformation between track frame and chair frame is governed by offset between track frame and chair frame (d_{chair}) and angular displacement of chair frame (ϕ).

$$\mathbf{T}_{\text{Chair}}^{\text{Track}} = \begin{bmatrix} cos\phi & -sin\phi & 0 & d_{chair} \\ sin\phi & cos\phi & 0 & 0 \\ sin\phi & cos\phi & 0 & 0 \\ 0 & 0 & 1 & 1 \end{bmatrix} \tag{32}$$

From Eqs. 26-31, the relation between the state matrix and the input matrix can be written as:

$$\begin{bmatrix} \dot{x}_t \\ \dot{y}_t \\ \dot{z}_t \\ \omega_x \end{bmatrix} = \mathbf{J}_{\text{i}} \begin{bmatrix} v_{lt} \\ v_{rt} \end{bmatrix} = \begin{bmatrix} \frac{1}{2}cos\psi cos\sigma & \frac{1}{2}cos\psi cos\sigma \\ \frac{1}{2}sin\psi cos\sigma & \frac{1}{2}sin\psi cos\sigma \\ \frac{1}{2}sin\sigma & \frac{1}{2}sin\sigma \\ \frac{1}{d} & -\frac{1}{d} \end{bmatrix} \begin{bmatrix} v_{lt} \\ v_{rt} \end{bmatrix} \tag{33}$$

Here, $\mathbf{J}_{\text{i}}$ is the Jacobian matrix. Given the input values of the velocities of the left and right tracks, the state of the robot can be determined.

The models that are developed within this section are implemented in the robot algorithm. Although numerous algorithms are simultaneously active for robot operation, the major algorithms that are within the scope of the paper are discussed. First of all, the staircase detection algorithm based on LIDAR data is actively seeking an approaching staircase (Algorithm 1). The LIDAR coordinates are converted into corner points with Harris Corner Detector [52]. As a polynomial curve is fitted within the points, the slope of the polynomial ascertains whether a staircase is approaching and if such obstacles are present then reports the dimension of such obstacles.

The main algorithm that is active is illustrated in Algorithm 2. This algorithm observes several functions for staircase detection and user command. As the staircase is not detected, the SCW has normal locomotion as per the user command. However, when a staircase is detected, the robot reaches the climbing pose by comparing the linear actuator feedback with the linear actuator goal from Eq. 20. This approach brings the robot to the climbing pose. The alignment of wheelchair tracks with the staircase is then checked and corrected using the rotational velocity given by Eq. 28. After the wheelchair is in an optimum position to climb, the wheelchair track motors are engaged until the wheelchair has traveled the total staircase length. At this point, the linear actuator corresponding to the balance wheel is expanded (s_1) until a slight change in seat angle is observed. The SCW is automatically brought to normal locomotion after the climbing process is complete.

2.3 Hardware Overview

The primary locomotion is based on the independently driven hub wheels actuated by brushless motors JQ-A2-8 (Changzhou Sunline Machinery Co.,Ltd, China). The motors can actuate a maximum load of 200 kg with a peak speed of 7 km/hr using a 24V supply. However, as the wheelchair approaches uneven terrain, hub wheels cannot proceed further. Therefore, rubber tracks powered by brushless motors Suntech-120W have been implemented to conveniently surmount the terrain such as the staircase. As evident from previous sections, two linear actuators are used to switch between the normal locomotion and tracked locomotion. It is performed by a planned motion between linear actuators 1 & 2, through the escalation of the chair base, which has hub wheels within the same link. Besides, linear actuators also serve as attitude angle adjustment system when maneuvering through different terrains. Finally, the power supply is provided by two Lithium Polymer batteries of capacity 20 Ampere-hour.

Since wheelchairs are supposed to be controlled by user, this robot as well relies on the user for the primary command which is provided with a joystick. However, as the task of ascending or descending the staircase demands careful adjustment of various angles, autonomy based on sensor data and previously described models have been implemented. For sensing the angular inclination, two inertial measurement unit (IMU) sensors of model Xsense MTi-G-710 have been placed, one within the seat frame and one within the track frame. The angular data from the sensors when fused with the angular data from the models can offer better control of the linear actuators and locomotion systems to provide safety and effective performance. The described system was designed and fabricated. The experimental performance of the system along the direction of the described models has been illustrated in the next section.

3 Experimental Evaluation and Results

As the primary goal of the robot was defined to maintain safety and accessibility, the performance of the robot while carrying a user across lower gradient staircase of 16° and a higher gradient staircase of 32° were observed and analyzed. The data from IMU sensors, LIDAR and potentiometers, that are built within the system, were recorded during the process of climbing up and climbing down for both the staircases.

For climbing down, Linear Actuators 1 and 2 are engaged so that the track and balance wheel forms contact with the ground, as shown in Fig. 10b. When the normal wheels are lifted, the track can successfully engage with the staircase and the balance wheel can be released once the tracks are fully in contact with the staircase as in Fig. 10c. As the wheelchair is transferred entirely on horizontal ground, normal wheels are engaged by manipulating the angle θ_2 as in Fig. 10d. The variation in heading angle across two frames can be observed in Fig. 12. Both the seat frame angle and the track frame angle which are almost the same, start to vary due to the linear displacement of both linear actuators in Fig. 15b. Finally, as the wheelchair approaches the

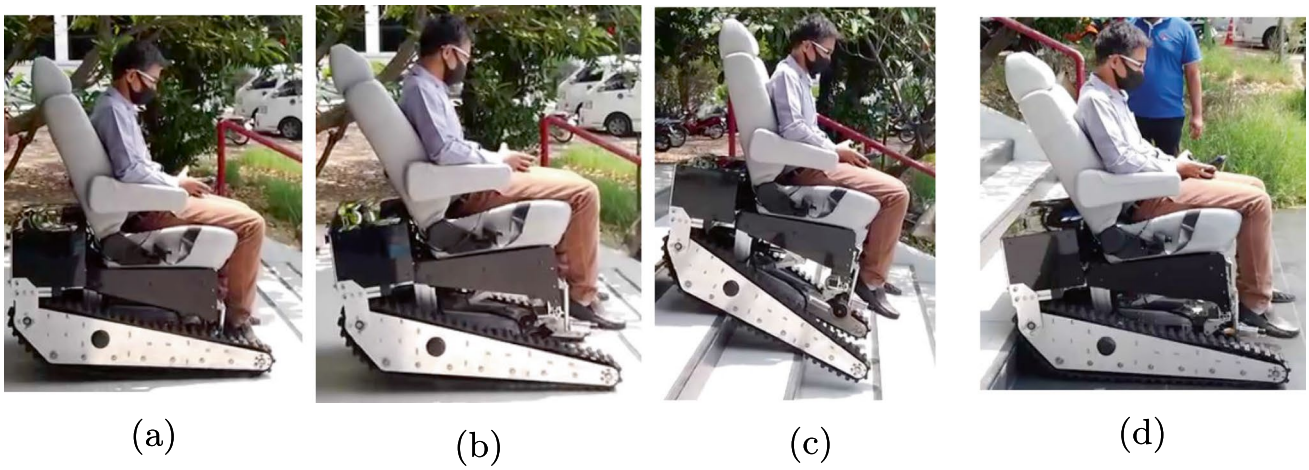

Fig. 10 Experimental Demonstration of the Stair Climbing Wheelchair during Climb-down Mode. (**a**) Motion Initiation, (**b**) Approaching staircase, (**c**) Climbing down, (**d**) Motion Completed

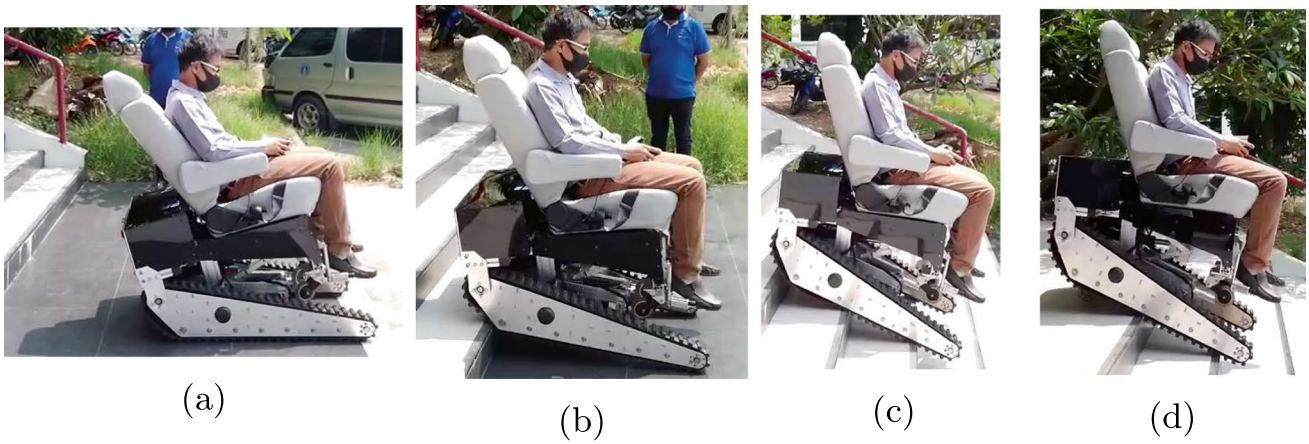

Fig. 11 Experimental Demonstration of the Stair Climbing Wheelchair during Climb-up Mode, (**a**) Initiation of Motion, (**b**) Approaching Staircase, (**c**) Climbing Up, (**d**), Releasing Balance Wheel and Completing Motion

horizontal ground, both the frame angles begin to coincide. Another major observation from Fig. 12a is the pose adjustment system that has been implemented. The angular variation produced by the track is attempted to nullify within the seat frame. As such, the pattern is similar but the

Similar to the climbing-down process, Fig. 11 illustrates the climbing-up process, which utilizes a sequence of motions. Unlike climb-down mode, the pose of engagement for climb-up mode is when the track is engaged and the balance wheel is unchanged. Due to this, just the seat angle can be observed to be decreasing initially in Figs. 11a and 12c. With this pose, the wheelchair approaches the staircase as illustrated in Fig. 11b and c. Finally, as the wheelchair approaches the end of the staircase, the balance wheel is engaged, as evident by the activity of Linear Actuator 2 towards the end of the motion in Fig. 12d. After the wheelchair maintains the posture with contact points as the front tip of the wheelchair and the balance wheel, the wheelchair is gradually manipulated back into the home position.

As discussed for the climb-down process, Fig. 12c demonstrates how the seat angle adjustment system tries to adapt variation in track angle by reflecting the pattern but tending to maintain zero mean angle for the safety of the user.

Also, since the vibration of the mobility devices tends to have an impact on the physical and psychological health of the user, a fourier transform of the angular data was conducted to isolate the frequency component of the signal as in [53]. The signal was transformed to the frequency domain and the amplitude of the signal was plotted against the frequency as in Fig. 14.

Finally, the experimental heading angle θ_1 was plotted against the estimated value using the linear actuator

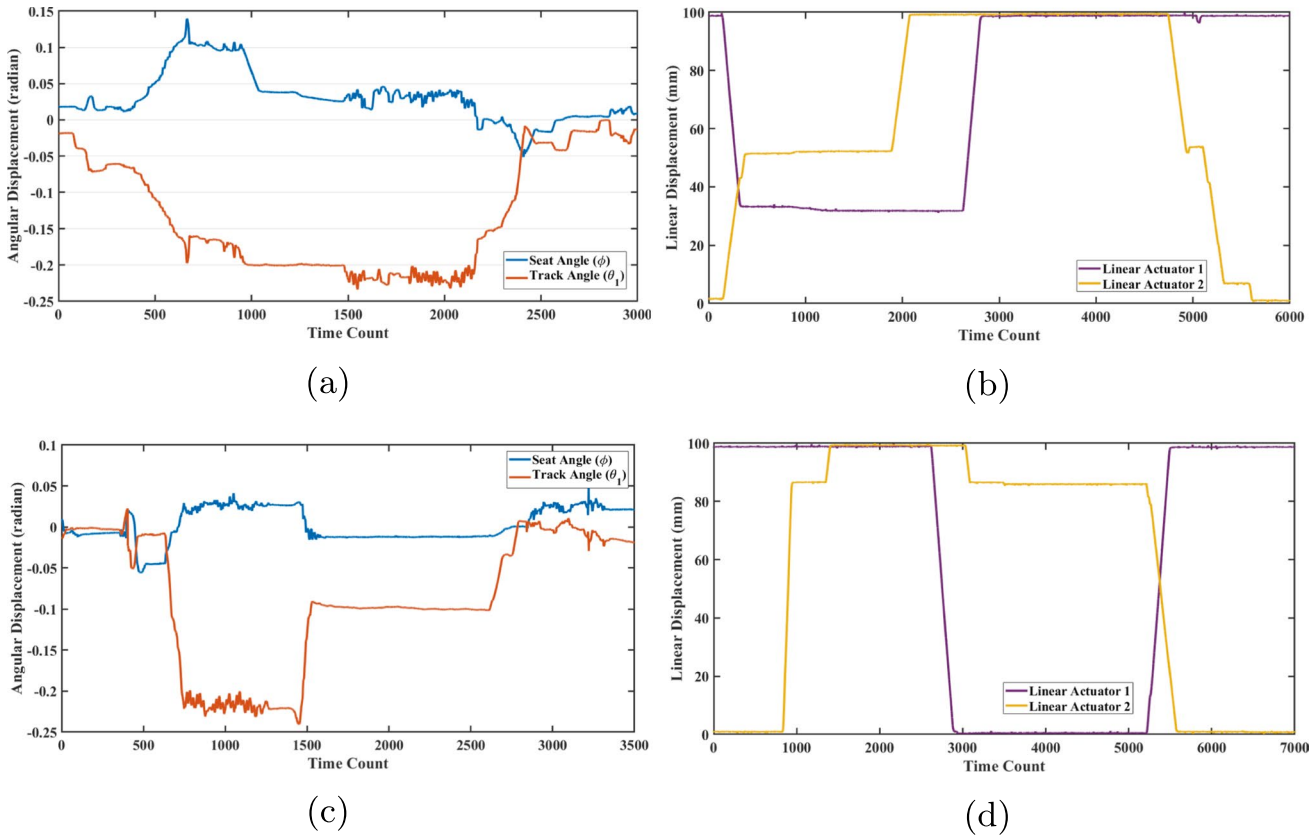

Fig. 12 Data from Experimental Demonstration during Climbing-up and Climbing-down Operation in 16° gradient staircase. (**a**) Angular Orientation of Seat and Track during Climbing-down Process, (**b**) Linear Actuator Feedback for Climbing-up Process, (**c**) Angular Orientation of Seat and Track during Climbing-down Process (**d**) Linear Actuator Feedback for Climbing-up Process

displacement data. This is to verify the method of pose adjustment and estimation, which combines linear actuator reading with the sensor reading.

4 Discussion

As this paper attempts to address the two key variables of accessibility and safety for mobility, they are the criteria for the evaluation of the results. The result from the experiment involving the user shows that the wheelchair can successfully execute the intended task and can move along a variety of terrains due to the kinematic and kinetic range of the design. Since staircases are among the intricate urban infrastructure elements, the ability to surpass this element means the staircase can also surmount other hindrances in the urban environment.

One of the major observations reported by few literature regarding the use of SCW has been the requirement of physical (handrails) or human assistance during the climbing process [25, 51]. However, due to the static and dynamic stability of the discussed model, no assistance is particularly required. Although the problem has been predominantly reported for the inverse pendulum mechanism, several similar models [15, 17] have substantially improved the stability. Since such mechanisms require sliding weight to balance the CG, the climb duration is longer. While [15] reported 24 seconds to surmount a single step, this model could climb up at 12 seconds and climb down at 6 seconds per step at a fully loaded condition. This is due to the autonomous pose adjustment system which operates in the background while the SCW climbs through different angles. As evident in Figs. 12a, c, 13a and c, the seat angle adjusts simultaneously as the track platform climbs the staircase.

In contrast to the three-wheeled cluster models [15, 18, 54], the proposed SCW model can overcome different kinds of obstacles including variable height staircase because of the tracked configuration. Also, when compared with the leg-wheel hybrid models, the proposed model performs climbing operations with a fewer DOF. While hybrid models such as [20, 22–24] have at least 6 DOFs, this paper introduces SCW with 4 DOF and can successfully perform the climbing operation. In addition, the robot consisting of legs requires meticulous motion planning operation involving inverse kinematics. This increases computational cost,

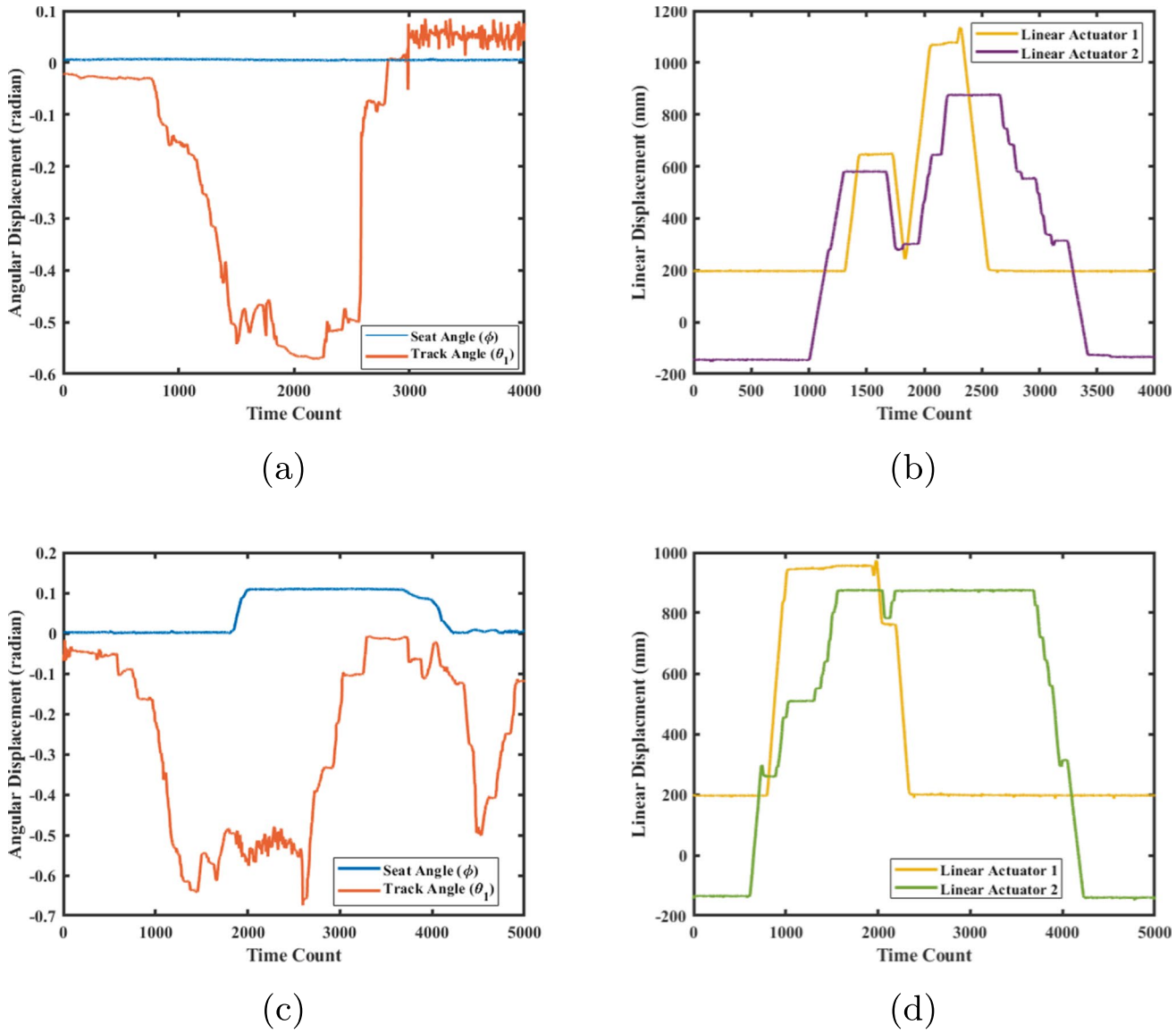

Fig. 13 Data from Experimental Demonstration during Climbing-up and Climbing-down Operation in 32° gradient staircase. (**a**) Angular Orientation of Seat and Track during Climbing-down Process, (**b**) Linear Actuator Feedback for Climbing-up Process, (**c**) Angular Orientation of Seat and Track during Climbing-down Process (**d**) Linear Actuator Feedback for Climbing-up Process

complexity and energy consumption, remarkably hampering the usability and commercial feasibility of such SCWs. Moreover, due to the leg, the overall length of the robot is bound to increase. For example, the length of SCWs such as [20] and [25] are longer than the standard size of a wheelchair. This impedes the wheelchair to make a turn and traverse through a confined space.

Regarding comfort, studies related to wheel-leg hybrid robot [19] and wheel cluster robot [12] suggest that the robot receives continuous oscillatory load while changing the stair. The load has high amplitude and frequency directly related to the speed of the wheelchair. This means the wheelchair has to compromise between speed and comfort. However, as Fig. 14 demonstrates, the discussed SCW receives low frequency, low amplitude vibration load even during the climbing process without compromising the speed. Therefore, compared with these SCWs, the model introduced in the paper has less DOF, does not require a complicated motion planning algorithm involving inverse kinematics, ensures a comfortable ride at optimum speed and is comparable with the standard wheelchair dimension.

However, many of the aforementioned shortcomings are irrelevant to the tracked SCWs, making track-wheel hybrid SCW one of the safest SCW [27]. Nevertheless, several limitations regarding the commercial track-wheel hybrid SCW have been reported [51]. The primary challenges for

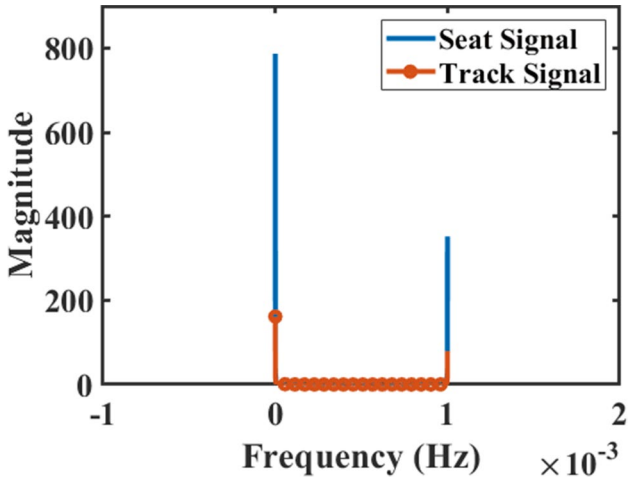

Fig. 14 Frequency Domain Analysis with Fourier Transform of Vibration Signals from IMU Sensors placed in Seat Link and Track Link

the user are track alignment with the staircase during climbing and transformation between normal locomotion and tracked locomotion. These limitations have been sufficed in this work with Algorithms 1 and 2. As the wheelchair approaches the staircase, the signal from LIDAR commands the system to initiate the climb mode. Within climb mode, as illustrated in Algorithm 2, if the climb direction of the wheelchair is not perpendicular to the staircase, the tracks produce differential motion until the distance of the staircase is the same for both the left and the right LIDAR. This semi-automated operation makes the process convenient and the requirement of any assistance is eschewed.

While [46–49] requires trajectory planning of the kinematic chain along with visual sensor-based pose estimation, such system require higher computational demand. Compared to that, this robot does not require trajectory planning. In contrast, this system considers the change in heading angle and calculates the corrective pose and provides necessary control command to the linear actuator to adjust with the changing terrain. As observed, this system ensures stable position by considering the changing attitude angle.

One of the threats for tracked SCW, that is widely reported is regarding the tip-over stability [20, 22, 27]. It has even been stated that the tracked SCW is suitable only for low-gradient staircase [15]. This is because of the factors such as fewer points of contact between the robot and the staircase, heavier robot and CG lying outside of track footprint while climbing [55]. To address the issue of lower contact points, two tracks with greater length are designed, so that during climbing at least three steps are in contact with the robot. Moreover, the tracks consist of rectangular profile grouser which increases the area of contact. To tackle the issue of weight, the use of steel is minimized and aluminum alloy is used as the main structural material, keeping the weight below 100 kilograms. Finally, to address the issue of CG, the majority of the mass of the robot including batteries, rotary motors and linear actuators accumulated towards the lower-rear end. Therefore, while climbing, the moment of force generated by the user mass in the clockwise direction is canceled by the moment of force produced towards the rear end in the anticlockwise direction. However, CG balance is also performed by adjusting the seat angle and maintaining it near or more than zero degree, as shown in Fig. 12a and c. Overall, based on the experimental observation and quantitative data, the estimation and adjustment system addressed the issue that are discussed in SCWs of different classes.

However, one of the concerns that emerge is regarding the unusual vibration that has low frequency but high amplitude [53]. This is detrimental to the comfort and wellness of the user. Therefore, this study realized the significance of the implementation of the vibration isolation or attenuation method. Moreover, the observation from frequency domain analysis in Fig. 14 shows that the reduction in amplitude of the vibration would produce a significant positive impact on the experience of the user, which means the damping effect compared to the spring effect in vibration suppression system is highly crucial for the reduction of the amplitude of vibration. Nevertheless, the magnitude of the signal is beyond the safety and comfort level, which is supposed to be reduced.

Finally, the comparison between the estimated heading angle and the actual heading angle in Fig. 15 showed the consistency of the proposed model in Eq. 10 and ultimately the Eq. 20. But if sensor fusion methods such as Kalman Filter or even Dempster-Shafer can be implemented, the quality of the result can be significantly improved. Regardless of that, the study shows the need for visual sensors such as LIDAR or depth cameras to effectively pre-define the terrain before the robot approaches for effective pose adjustment. The result from the visual sensors, when combined with the sensor-based models as discussed in this paper, contributes highly to address the problem of accessibility and safety.

5 Conclusion

While PMDs such as SCWs are convenient and prevalent for ambulatory assistance, the issues of safety and accessibility are still the major concerns. Among the different modes of locomotion, this paper introduced and discussed a wheel-track hybrid SCW. A kinematic model and sensor system consisting of IMU and LIDAR were combined to develop an algorithm that could ensure semi-autonomous operation for easy and safe climbing and transitioning process. The results suggest that the wheelchair can

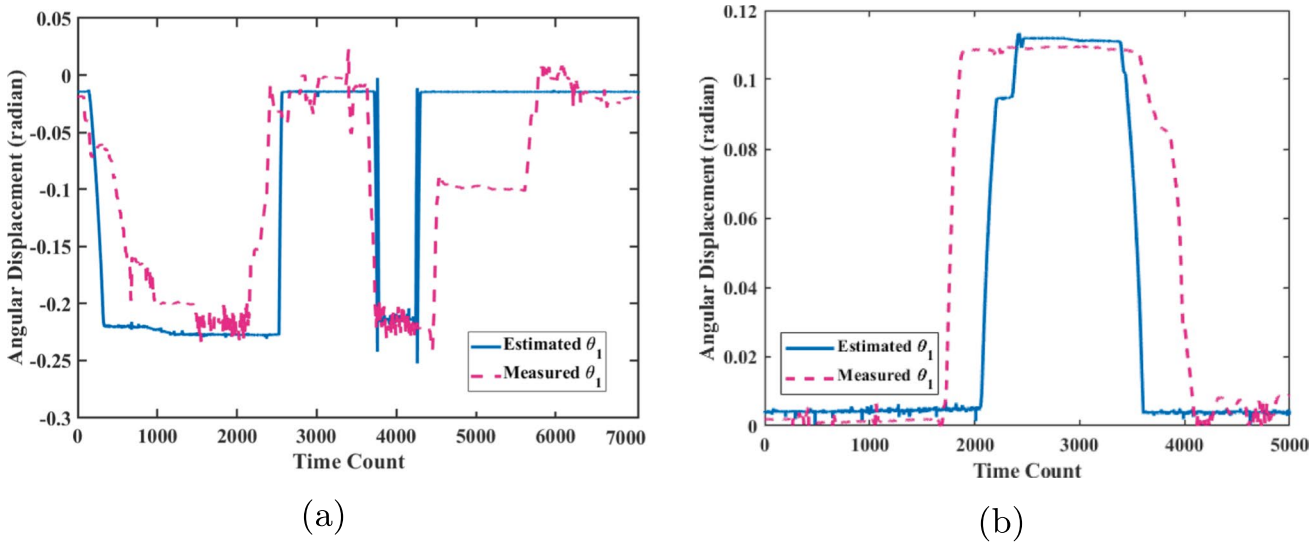

Fig. 15 Estimation of the Angular Tilt with Feedback from Linear Actuator and Actual Sensor Measurement (**a**) Angular Estimation in 16° (**b**) Angular Estimation in 32°

fulfill the intended objective. For the future direction of the research, an advanced algorithm would be adapted to autonomously visualize the terrain and adopt the pose accordingly. Secondly, human-robot interaction would be developed further by introducing technologies such as brain-computer interface and compliance control method. Since basic vibration has been studied and assessed, this research indicates the requirement of an effective suspension system. Finally, other shortcomings that were observed and mentioned in this paper would be implemented in future iterations for making the wheelchair safe, comfortable and effective for the user.

Supplementary Information The online version contains supplementary material available at https://doi.org/10.1007/s10846-022-01765-3.

Acknowledgements The authors would like to thank the members of Center for Biomedical and Robotics Technology (BART LAB), Mahidol University for their valuable support to the research. The authors specially acknowledge the contribution of Mr. Amorchai Khawkhom, whose efforts have helped materialize this project.

Author Contributions JS conceptualized the project along with the design. BS worked on the mechanical design, development, manufacturing and assembly. BMP developed the dynamic model and control system. KB worked towards the software development and performance of the robotic system. Manuscript was prepared by BS, reviewed and corrected by BMP and supervised by JS.

Funding This research is supported by the National Research Council of Thailand (Funding No.: NRCT-MHESRI 34/2562) under the title "Intelligent Robotic Wheelchair for Elderly and Disable Persons to Use in Daily Life and Stair Climbing Project".

Data Availability Data sharing is not applicable to this article as the entire dataset generated during the study has been graphically illustrated in Figs. 12 to 15.

Declarations

Ethical approval Not Applicable

Consent to Participate Informed consent has been received from the involved participants.

Consent to Publish The participant involved is a member of the development team and consent has been obtained regarding the use of their image.

Competing Interest The authors declare no competing interest.

References

1. Grand View Research: Personal mobility devices market size, share, and trends analysis report by product (Walking Aids, Wheelchairs, Scooters), By Region (Europe, APAC, North America, MEA), And Segment Forecasts, 2021–2028. Technical report, San Fransisco (2021)
2. Edwards, K., McCluskey, A.: A survey of adult power wheelchair and scooter users. Disabil. Rehabil.: Assist. Technol. **5**(6), 411–419 (2010). https://doi.org/10.3109/17483101003793412
3. Ferreira, A.F., Leite, A.D., Pereira, L.d.F., Neves, J.M.d.J., de Oliveira Pinheiro, M.G., Chang, S.K.J.: Wheelchair accessibility of urban rail systems: Some preliminary findings of a global overview. IATSS Research (xxxx) (2021). https://doi.org/10.1016/j.iatssr.2021.01.003
4. Belcher, M.J.H., Frank, A.O.: Survey of the use of transport by recipients of a regional Electric Indoor/Outdoor Powered (EPIOC) wheelchair service. Disabil. Rehabil. **26**(10), 563–575 (2004). https://doi.org/10.1080/09638280410001684055
5. Shin, G.W., Lee, K.J., Park, D., Lee, J.H., Yuri, M.H.: Personal mobility device and user experience: A state-of-the-art literature review. Proceedings of the Human Factors and Ergonomics Society **2**(21), 1336–1337 (2018). https://doi.org/10.1177/1541931218621305

6. Tao, W., Xu, J., Liu, T.: Electric-powered wheelchair with stair-climbing ability. Int. J. Adv. Robot. Syst. **14**(4), 1–13 (2017). https://doi.org/10.1177/1729881417721436
7. Yuan, J., Hirose, S.: Research on leg-wheel hybrid stair-climbing robot, zero carrier. In: 2004 IEEE International Conference on Robotics and Biomimetics, pp. 654–659 (2004). https://doi.org/10.1109/ROBIO.2004.1521858
8. Wang, H., He, L., Li, Q., Zhang, W., Zhang, D., Xu, P.: Research on a kind of leg-wheel stair-climbing wheelchair. 2014 IEEE International Conference on Mechatronics and Automation, IEEE ICMA 2014, 2101–2105 (2014). https://doi.org/10.1109/ICMA.2014.6886028
9. Behera, P.K., Gupta, A.: Novel design of stair climbing wheelchair. J. Mech. Sci. Technol. **32**(10), 4903–4908 (2018). https://doi.org/10.1007/s12206-018-0938-6
10. Liu, J., Wu, Y., Guo, J., Chen, Q.: High-order sliding mode-based synchronous control of a novel stair-climbing wheelchair robot. J. Control Sci. Eng. **2015** (2015). https://doi.org/10.1155/2015/680809
11. Lawn, M.J., Ishimatsu, T.: Modeling of a stair-climbing wheelchair mechanism with high single-step capability. IEEE Trans. Neural Syst. Rehabil. Eng. **11**(3), 323–332 (2003). https://doi.org/10.1109/TNSRE.2003.816875
12. Quaglia, G., Franco, W., Oderio, R.: Wheelchair.q, a motorized wheelchair with stair climbing ability. Mech. Mach. Theory **46**, 1601–1609 (2011). https://doi.org/10.1016/j.mechmachtheory.2011.07.005
13. Quaglia, G., Franco, W., Nisi, M.: Kinematic analysis of an electric stair-climbing wheelchair. Ing. Univ. **21** (2017). https://doi.org/10.11144/Javeriana.iyu21-1.kaes
14. Quaglia, G., Nisi, M.: Design of a self-leveling cam mechanism for a stair climbing wheelchair. Mech. Mach. Theory **112**, 84–104 (2017). https://doi.org/10.1016/j.mechmachtheory.2017.02.003
15. Onozuka, Y., Tomokuni, N., Murata, G., Shino, M.: Dynamic stability control of inverted-pendulum-type robotic wheelchair for going up and down stairs. IEEE International Conference on Intelligent Robots and Systems, 4114–4119 (2020). https://doi.org/10.1109/IROS45743.2020.9341242
16. Onozuka, Y., Tomokuni, N., Murata, G., Shino, M.: Attitude control of an inverted-pendulum-type robotic wheelchair to climb stairs considering dynamic equilibrium. ROBOMECH J. **7** (2020). https://doi.org/10.1186/s40648-020-00171-4
17. Jamin, N.F., Ghani, N.M.A., Ibrahim, Z.: Movable payload on various conditions of two-wheeled double links wheelchair stability control using enhanced interval type-2 fuzzy logic. IEEE Access **8**, 87676–87694 (2020). https://doi.org/10.1109/ACCESS.2020.2991433
18. Prajapat, M., Sikchi, V., Shaikh-Mohammed, J., Sujatha, S.: Proof-of-concept of a stair-climbing add-on device for wheelchairs. Med. Eng. Phys. **85**, 75–86 (2020). https://doi.org/10.1016/j.medengphy.2020.09.013
19. Castillo, B.D., Kuo, Y.F., Chou, J.J.: Novel design of a wheelchair with stair climbing capabilities. ICIIBMS 2015 - International Conference on Intelligent Informatics and Biomedical Sciences 2(1), 208–215 (2016). https://doi.org/10.1109/ICIIBMS.2015.7439508
20. Ning, M., Yu, K., Zhang, C., Wu, Z., Wang, Y.: Wheelchair design with variable posture adjustment and obstacle-overcoming ability. J. Braz. Soc. Mech. Sci. Eng. **43**(4) (2021). https://doi.org/10.1007/s40430-021-02921-w
21. Mostyn, V., Krys, V., Kot, T., Bobovsky, Z., Novak, P.: The synthesis of a segmented stair-climbing wheel. Int. J. Adv. Robot. Syst. **15**(1), 1–11 (2018). https://doi.org/10.1177/1729881417749470
22. Sugahara, Y., Yonezawa, N., Kosuge, K.: A novel stair-climbing wheelchair with transformable wheeled four-bar linkages. IEEE/RSJ 2010 International Conference on Intelligent Robots and Systems, IROS 2010 - Conference Proceedings, 3333–3339 (2010). https://doi.org/10.1109/IROS.2010.5648906
23. Candiotti, J.L., Daveler, B.J., Kamaraj, D.C., Chung, C.S., Cooper, R., Grindle, G.G., Cooper, R.A.: A heuristic approach to overcome architectural barriers using a robotic wheelchair. IEEE Transactions on Neural Systems and Rehabilitation Engineering : A Publication of the IEEE Engineering in Medicine and Biology Society **27**, 1846–1854 (2019). https://doi.org/10.1109/TNSRE.2019.2934387
24. Hinderer, M., Friedrich, P., Wolf, B.: An autonomous stair-climbing wheelchair. Robot. Auton. Syst. **94**, 219–225 (2017). https://doi.org/10.1016/j.robot.2017.04.015
25. Baishya, N.J., Bhattacharya, B., Ogai, H., Tatsumi, K.: Analysis and design of a minimalist step climbing robot. Appl. Sci. (Switzerland) **11** (2021). https://doi.org/10.3390/app11157044
26. Sasaki, K., Eguchi, Y., Suzuki, K.: Stair-climbing wheelchair with lever propulsion control of rotary legs. Adv. Robot. **34**, 802–813 (2020). https://doi.org/10.1080/01691864.2020.1757505
27. Verma, A., Shrivastava, S., Ramkumar, J.: Mapping wheelchair functions and their associated functional elements for stair climbing accessibility: a systematic review. Disabil. Rehabil.: Assist. Technol (2022). https://doi.org/10.1080/17483107.2022.2075476
28. Yu, S., Wang, T., Wang, Z., Wang, Y., Yao, C., Li, X.: Original design of a wheelchair robot equipped with variable geometry single tracked mechanisms. Int. J. Robotics Autom. **30** (2015)
29. Tao, W., Jia, Y., Liu, T., Yi, J., Wang, H., Inoue, Y.: A novel wheel-track hybrid electric powered wheelchair for stairs climbing. J. Adv. Mech. Des. Syst. Manuf. **10**(4), 1–21 (2016). https://doi.org/10.1299/JAMDSM.2016JAMDSM0060
30. Jorge, A.A., Riascos, L.A.M., Miyagi, P.E.: Modelling and control strategies for a motorized wheelchair with hybrid locomotion systems. J. Braz. Soc. Mech. Sci. Eng. **43**(1), 1–15 (2021). https://doi.org/10.1007/s40430-020-02730-7
31. Thamel, S.R., Munasinghe, R., Lalitharatne, T.: Motion planning of novel stair-climbing wheelchair for elderly and disabled people. MERCon 2020 - 6th International Multidisciplinary Moratuwa Engineering Research Conference, Proceedings, 590–595 (2020). https://doi.org/10.1109/MERCon50084.2020.9185273
32. Ciabattoni, L., Ferracuti, F., Freddi, A., Iarlori, S., Longhi, S., Monteriù, A.: Human-in-the-loop approach to safe navigation of a smart wheelchair via brain computer interface, vol. 725, pp. 197–209. Springer, (2021). https://doi.org/10.1007/978-3-030-63107-9_16
33. Li, Z., Li, X., Li, Q., Su, H., Kan, Z., He, W.: Human-in-the-loop control of soft exosuits using impedance learning on different terrains. IEEE Transactions on Robotics, 1–10 (2022). https://doi.org/10.1109/TRO.2022.3160052
34. Yu, X., Li, B., He, W., Feng, Y., Cheng, L., Silvestre, C.: Adaptive-constrained impedance control for human-robot co-transportation. IEEE Transactions on Cybernetics, 1–13 (2021). https://doi.org/10.1109/TCYB.2021.3107357
35. Yu, X., He, W., Li, Q., Li, Y., Li, B.: Human-robot co-carrying using visual and force sensing. IEEE Trans. Ind. Electron. **68**, 8657–8666 (2021). https://doi.org/10.1109/TIE.2020.3016271
36. Huang, Q., Zhang, Z., Yu, T., He, S., Li, Y.: An EEG-/EOG-based hybrid brain-computer interface: Application on controlling an integrated wheelchair robotic arm system. Front. Neurosci. **13** (2019). https://doi.org/10.3389/fnins.2019.01243
37. Fuke, Y., Krotkov, E.: Dead reckoning for a lunar rover on uneven terrain. Proceedings - IEEE International Conference on Robotics and Automation **1**, 411–416 (1996). https://doi.org/10.1109/robot.1996.503811
38. Yu, J.X., Cai, Z.X., Duan, Z.H., Zou, X.B.: Design of dead reckoning system for mobile robot. Journal of Central South University of Technology (English Edition) **13**(5), 542–547 (2006). https://doi.org/10.1007/s11771-006-0084-7
39. Huang, X., Wang, J.: Real-time estimation of center of gravity position for lightweight vehicles using combined AKF-EKF method. IEEE Trans. Veh. Technol. **63**(9), 4221–4231 (2014). https://doi.org/10.1109/TVT.2014.2312195

40. Mourikis, A.I., Trawny, N., Roumeliotis, S.I., Helmick, D.M., Matthies, L.: Autonomous stair climbing for tracked vehicles. Int. J. Robot. Res. **26**(7), 737–758 (2007). https://doi.org/10.1177/0278364907080423
41. Sakai, Y., Lu, H., Tan, J.K., Kim, H.: Environment recognition for electric wheelchair based on YOLOv2. ACM International Conference Proceeding Series, 112–117 (2018). https://doi.org/10.1145/3278229.3278231
42. Ullah, Z., Xu, Z., Lei, Z., Zhang, L.: A robust localization, slip estimation, and compensation system for WMR in the indoor environments. Symmetry **10**(5), 1–20 (2018). https://doi.org/10.3390/sym10050149
43. Sidharthan, R.K., Kannan, R., Srinivasan, S., Balas, V.E.: Stochastic wheel-slip compensation based robot localization and mapping. Adv. Electr. Comput. Eng. **16**(2), 25–32 (2016). https://doi.org/10.4316/AECE.2016.02004
44. Sharma, B., Pillai, B.M., Suthakorn, J.: Live displacement estimation for rough terrain mobile robot: Bart lab rescue robot. In: 2021 International Siberian Conference on Control and Communications (SIBCON), pp. 1–6 (2021). https://doi.org/10.1109/SIBCON50419.2021.9438919
45. Pillai, M.B., Nakdhamabhorn, S., Borvorntanajanya, K., Suthakorn, J.: Enforced acceleration control for dc actuated rescue robot. In: 2016 XXII International Conference on Electrical Machines (ICEM), pp. 2640–2648 (2016). https://doi.org/10.1109/ICELMACH.2016.7732894
46. Botta, A., Bellincioni, R., Quaglia, G.: Autonomous detection and ascent of a step for an electric wheelchair. Mechatronics **86** (2022). https://doi.org/10.1016/j.mechatronics.2022.102838
47. Chocoteco, J., Morales, R., Feliu, V.: Improving the climbing/descent performance of stair-climbing mobility systems confronting architectural barriers with geometric disturbances. Mechatronics **30**, 11–26 (2015). https://doi.org/10.1016/j.mechatronics.2015.06.001
48. Chocoteco, J., Morales, R., Feliu, V., Sanchez, L.: Trajectory planning for a stair-climbing mobility system using laser distance sensors. IEEE Syst. J. **10**, 944–956 (2016). https://doi.org/10.1109/JSYST.2014.2309477
49. Ikeda, H., Toyama, T., Maki, D., Sato, K., Nakano, E.: Cooperative step-climbing strategy using an autonomous wheelchair and a robot. Robot. Auton. Syst. **135** (2021). https://doi.org/10.1016/j.robot.2020.103670
50. Wang, J., Wang, T., Yao, C., Li, X., Wu, C.: Active tension control for wt wheelchair robot by using a novel control law for holonomic or nonholonomic systems. Math. Probl. Eng. **2013** (2013). https://doi.org/10.1155/2013/236515
51. Laffont, I., Guillon, B., Fermanian, C., Pouillot, S., Even-Schneider, A., Boyer, F., Ruquet, M., Aegerter, P., Dizien, O., Lofaso, F.: Evaluation of a stair-climbing power wheelchair in 25 people with tetraplegia. Arch. Phys. Med. Rehabil. **89**, 1958–1964 (2008). https://doi.org/10.1016/j.apmr.2008.03.008
52. Harris, C.G., Stephens, M.J.: A combined corner and edge detector. In: Alvey Vision Conference (1988)
53. Prażnowski, K., Mamala, J., Śmieja, M., Kupina, M.: Assessment of the road surface condition with longitudinal acceleration signal of the car body. Sensors (Switzerland) **20**(21), 1–19 (2020). https://doi.org/10.3390/s20215987
54. Riascos, L.A.M.: A low cost stair climbing wheelchair. IEEE International Symposium on Industrial Electronics, 627–632 (2015). https://doi.org/10.1109/ISIE.2015.7281541
55. Yu, S., Wang, T., Wang, Y., Zhi, D., Yao, C., Li, X., Wang, Z., Luo, Y., Wang, Z.: A tip-over and slippage stability criterion for stair-climbing of a wheelchair robot with variable geometry single tracked mechanism. In: 2012 IEEE International Conference on Information and Automation, pp. 88–93 (2012). https://doi.org/10.1109/ICInfA.2012.6246788

Bibhu Sharma receivedthe M.E. in Biomedical Engineering from the Faculty of Engineering, MahidolUniversity, Thailand and B.E. in Mechanical Engineering from KathmanduUniversity, Nepal. He is currently involved in research at the Center ofBiomedical and Robotics Technology (BART LAB), Department of BiomedicalEngineering, Faculty of Engineering, Mahidol University, Thailand. In past, hehas worked as a Design Engineer for Honda R&D, Tochigi, Japan. He has beeninvolved with research pertaining to medical robotics, biomechanics, softrobotics and rough-terrain robotics along the direction of design, dynamics,and control.

Branesh M. Pillai received the bachelor's degree from AnnaUniversity, India, in 2007, the master's degree by research in control systemsfrom the University of Moratuwa, in 2013, and the Ph.D. degree in biomedicalengineering (medical robotics) from Mahidol University, Thailand, in 2019. Heis currently a Faculty Member at the Center for Biomedical and RoboticsTechnology (BART LAB), Faculty of Engineering, Mahidol University. His researchinterests include medical robotics and the work-related to robot-assistedsurgery, advanced motion control, biomechanics, and rough terrain rescue robot.

Korn Borvorntanajanya received the master's (by Research) degree inmedical robotics and the bachelor's degree from the Department of BiomedicalEngineering, Mahidol University, Thailand, in 2013 and 2018, respectively. Heis currently a Researcher at the Center for Biomedical and Robotics Technology(BART LAB), Faculty of Engineering, Mahidol University. His research interestsinclude medical robotics, human–robot interaction (HRI), digital signal andimage processing, SLAM & navigation, and control systems.

Jackrit Suthakorn (Member, IEEE) received the bachelor's degree inmechanical engineering from Mahidol University, Thailand, in 1995, the master'sdegree in control engineering from Michigan Technological University, Houghton,MI, USA, in 1998, and the Ph.D. degree in robotics from Johns HopkinsUniversity, Baltimore, MD, USA, in 2003. He had established the Center forBiomedical and Robotics Technology (BART LAB), the first focused MedicalRobotics Research Group in Thailand, since 2004. In 2006, he and his colleagueshad established the Department of Biomedical Engineering, Mahidol University,as the first and only the Biomedical Engineering Department in Thailand, whichwas quickly become well-known among the top engineering departments in Thailand. He is currently the Dean of Engineering, Faculty of Engineering, Mahidol University, and the President of the Thailand's Engineering Deans Association, which leads the Council of Engineering Deans of Thailand. His research interests include aiming for medical robotics surgical robotics in various applications, such as neuro surgery, breast biopsy, orthopedic surgery, rehabilitation robotics, such as lower limb exoskeletal, elderly carrying robotic systems, hospital service and tele-medicine robotics, such as autonomous drug delivery robots, tele-med mobile robot, and VR surgical training systems. He was one of the Founder of Thai Robotics Society (TRS), in 2004, which later on, he was selected to be the President of Thai Robotics Society, from 2007 to 2010. Currently, he also serves as a Trustee of the International RoboCup Federation and the Vice President of RoboCup AsiaPacific (RCAP). Recently, he is the Chair of IEEE RAS Thailand Chapter.